THE JOURNAL OF PHYSICAL CHEMISTRY A

Article

pubs.acs.org/JPCA

Computational Study of Ways by Which *exo*-Silatranes Might Be Prepared

Published as part of The Journal of Physical Chemistry virtual special issue "Mark S. Gordon Festschrift".

Carolynn Hoeksema, Marc J. Adler, and Thomas M. Gilbert*

Department of Chemistry & Biochemistry, Northern Illinois University, DeKalb, Illinois 60115, United States

Supporting Information

ABSTRACT: *exo*-Silatranes involve cage structures where the nitrogen lone pair points away from the cage rather than into it. This distinguishes them from the well-established *endo*-silatranes. *exo*-Silatranes have not been observed experimentally, consistent with a significant benefit to silicon−nitrogen interactions inside the cages as suggested for *endo*-silatranes. Identifying examples of *exo*-silatranes would prove useful in understanding Si−N interactions, as they would represent the "no interaction" extreme of the spectrum. We have found four means by which *exo*-silatranes might be synthesized: (1) employing smaller cages; (2) employing constrained rings to stiffen the cage backbones; (3) employing steric interactions to enhance preference for the less crowded *exo*-geometry around nitrogen; (4) modifying the Lewis acidity and basicity of the silicon and nitrogen so significantly as to remove their desire to interact. The preference for *exo* geometries is established using the parameter Δ, representing the distance between the nitrogen atom and the least-squares plane containing the adjacent carbon atoms. In some cases, Δ values for *exo*-silatranes are greater than 0.3 Å. In others, they are near zero, indicating a nearly planar nitrogen atom. There are no obvious structural markers besides Δ that distinguish between *exo*- and *endo*-silatranes.

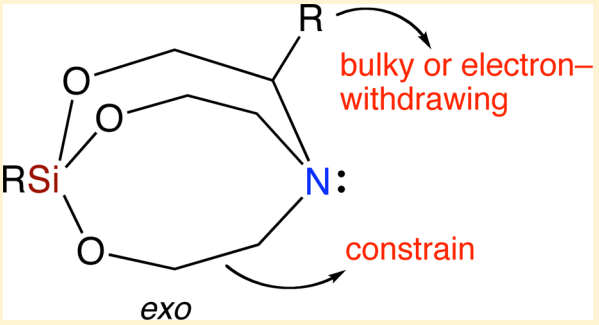

INTRODUCTION

Silatranes, $RSi[OCR_2CR_2]_3N$,[1] have proved intriguing since their initial syntheses and structural examinations.[2] By far the issue attended most is that of the degree of covalent interaction between the apical silicon and nitrogen atoms. Although structural studies show without exception Si−N distances significantly shorter than the sum of the van der Waals radii,[2] an observation originally thought to imply significant covalent interaction between the Si and N atoms, recent X-ray diffraction electron density,[3] and photoelectron spectroscopy[4] studies indicate an essentially electrostatic interaction. Nonetheless, a degree of experimental[5,6] and computational[7−9] support for the covalent interaction view comes from observations that Si−N distances (and presumably the degree of interaction) correlate with the electron withdrawing/donating properties of the R substituent. However, the flat potential energy surface for Si/N positioning implied by differences between solid-state and gas-phase[10,11] Si−N distances makes the correlation tenuous though intuitively likely.

A more basic observation supporting the view that Si/N interactions are significant is that all structural studies show what is termed the "*endo*" geometry at nitrogen; that is, the NC_3 moiety is pyramidalized toward the silicon (Figure 1). In VSEPR terms, the N lone pair points toward the silicon, a situation characterized as an Si Lewis acid/N Lewis base

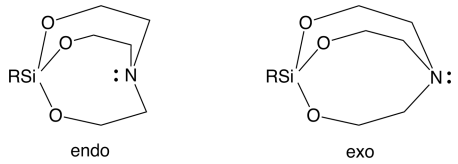

Figure 1. Silatranes with *endo* and *exo* geometries at the nitrogen atom.

interaction. No examples of "*exo*" silatranes, with the nitrogen geometry inverted with respect to the *endo* conformer, have been discovered. Indeed, potential energy surface studies associated with Si−N distances/interaction in several silatranes have consistently provided single minimum curves consistent with computational optimization results, preferring *endo* structures.[7c,12] Such observations further support the view that the silicon and nitrogen atoms interact sufficiently to dictate structural outcomes.

We were intrigued by the lack of extant *exo* conformers and wondered if modeling studies might point a way to their syntheses. As one can view *exo*/*endo* isomers of particular molecules as structurally elusive "bond stretch isomers",[13−15] it was of additional interest to see if potential energy curves for

Received: September 18, 2016
Revised: November 1, 2016
Published: November 2, 2016

DOI: 10.1021/acs.jpca.6b09346
J. Phys. Chem. A 2016, 120, 9315−9323

putative systems might display double minima, thus presenting the possibility of preparing such isomers. We were further motivated by recent modeling studies[16,17] that suggested that some phosphasilatranes $RSi[OCR_2CR_2]_3P$ showed sizable preferences for *exo* geometries at phosphorus, in stark contrast to observations for silatranes. Finally, we wondered if a silatrane cage might stabilize the tertiary nitrogen atom in a planar geometry, something theorized in NR_3 molecules where R is extremely bulky, but not unambiguously observed.[18,19] Compounds containing planar nitrogen atoms are of experimental and theoretical interest owing to the significant substituent crowding involved, their utility as models for transition states for amine inversion processes, and their potential to display near-diradical behavior.[18,20,21]

We therefore undertook modeling studies with the goals of identifying silatranes that would exhibit *exo* nitrogen geometries, of determining whether such silatranes would display bond stretch isomerism, and of employing localization techniques to distinguish Si−N interactions and the lack thereof between *exo* and *endo* conformers. We have discovered several examples of *exo* silatranes that should clearly be preferred to *endo* ones, involving diverse approaches including limiting the flexibility of the cage backbone (**5**, **6**, **11ax**) and modifying the Lewis basicity of the nitrogen (**15**, **19H+2**, **20H+2**, and **20H+3**). Not all *exo* isomers appear to lend themselves to ready syntheses, but some do (**11ax** and the **19**/**20** series, in particular), and in our view are worth exploring. We were unable to identify molecules that might be bond stretch isomers but discovered some that might contain planar nitrogen atoms.

COMPUTATIONAL METHODS

Optimizations and frequency analyses were performed using the GAMESS[22,23] and Gaussian (G09)[24] suites. All molecules examined were initially fully optimized without constraints at either the HF/6-31+G(d,p) or the M06-2X[25]/6-31+G(d) level. Molecules that adopted symmetric or near-symmetric structures were reoptimized constrained to that symmetry (often C_3). A sizable integration grid (99 radial shells, 590 angular points) was used in all cases. *Exo* starting structures were typically employed; when the optimization procedure found an *exo* minimum stationary point, the molecule was reoptimized beginning with an *endo* starting structure. This ensured that *exo* structures were justifiably global minima. Structures of interest were then reoptimized at the M11[26]/6-311+G(d,p) level. Analytical frequency analyses at this level demonstrated that the structures were minima (no imaginary frequencies), and provided zero-point energies (ZPEs), which were used unscaled when relative energies were calculated. Several structures were reoptimized at the ωB97X-D[27]/6-311+G(d,p) and MP2[28]/6-311+G(d,p) levels as checks on the M11 results and to compare effects of the different ways the three models capture dispersion effects. Because the Si−N interaction is dative and long-range, it is critical to model dispersion effects well. All results are stored as Supporting Information; as the M11/6-311+G(d,p) results were representative, only these are discussed below.

The Mercury program[29] was used to calculate least-squares planes (denoted C3 in the Tables below) involving the nitrogen-bound carbon atoms and to determine Si−C3 and Si−N distances (Figure 2). Figure 5 was generated using the Molecule for Macintosh program.[30]

Bond critical points (BCPs) and bond paths (BPs) were located using the AIMAll program,[31] which implements the Quantum Theory of Atoms In Molecules (QTAIM) theory developed by Bader and co-workers.[32−34] Test calculations were undertaken using wave functions obtained from reoptimizations of silatranes **8** and **12** at the M11/basis set levels, where basis set 6-311+G(d,p) (6d, 10f),[35] aug-cc-pVTZ,[36−38] pcseg-2, aug-pcseg-2, and pcseg-3.[39] The results showed erratic behavior, in that some model chemistries located BCPs between Si and N, whereas others did not (see Supporting Information Table S4 showing this, and related results described below). The default for the AIMAll program is to generate a BCP (and corresponding BP) wherever the requisite (3, −1) condition is met and $\rho > 0$. This can result in observation of artifactual BCPs resulting from imperfections in the ability of the model chemistry to properly characterize the electron density of the molecule; examples traced to basis set incompleteness exist,[32−34] which is why we examined multiple basis sets. Location of a BCP correlated weakly with the ζ level of the basis set, but not with the presence/absence of diffuse functions, the Si−N distance or the value of Δ. Moreover, even in cases where an Si−N BCP was located, the ρ value for this was often less than that determined for "nonbonding" critical points located. For example, for fluorinated **8** at the M11/aug-cc-pVTZ level, an Si−N BCP was located with $\rho = 0.015$. BCPs were also located between backbone methylene H and F substituents, also with $\rho = 0.015$. Similarly, for **12** at the M11/pcseg-2 level, an Si−N BCP was located with $\rho = 0.015$, but H···H BCPs were also located between backbone methylene H substituents with $\rho = 0.017$ or 0.020, depending on pairing. Neither the H···F interactions in **8** nor the H···H interactions in **12** would be characterized as bonds in the conventional sense. These examples point to any BCP in these silatranes with $\rho <$ 0.02 or so as being artifactual.[40] All ρ values for Si−N BCPs located at all model chemistries tested fell below this cutoff, so in our view the BCPs are probably artifacts. All other molecules examined using QTAIM approaches were reoptimized solely at the M11/aug-cc-pVTZ and pcseg-3 levels. We report below only results from the M11/pcseg-3 model chemistry, as this basis set was developed specifically for DFT calculations, employed the most extensive basis set, and gave the best agreement for experiment for atomization energies,[39] and so was most likely to give reliable data.

RESULTS AND DISCUSSION

We identified four chemical features that might allow syntheses of *exo* silatranes.

1. Smaller Cages. An obvious approach to forcing the nitrogen to adopt the *exo* geometry is to make the cage rings sufficiently small that adopting the *endo* geometry induces unacceptable ring strain. Obvious candidates include what we term "silatanes", as an extension of the commonplace "atrane" terminology.[41−43] Silatanes are molecules of formula $XSi(OCR_2)_3N$, a [2,2,2] cage composed of six-membered rings (Figure 2). One can view silatanes as structural analogues of [2,2,2]-bicyclooctane or DABCO, which exist solely as *exo* conformers. Silatanes are poorly studied; a literature search found only two reports, a 1988 Chinese structure/toxicity computational study of an array of examples and a 2009 French patent dealing with a silatane containing a thiol bound to silicon.[44,45] This further motivated examining examples here.

The silatanes examined contained neutral, electron-withdrawing, and electron-donating substituents on silicon (Figure 2, left). Substitution had the expected effects (Table 1): compared to the parent **1**, electron-richer **2** exhibits longer Si−

DOI: 10.1021/acs.jpca.6b09346
J. Phys. Chem. A 2016, 120, 9315−9323

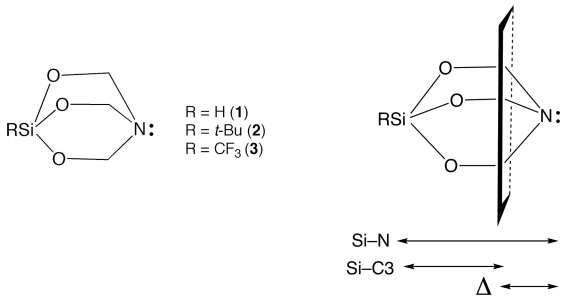

Figure 2. Skeleton picture of a silatane (left) and graphic (right) showing the least-squares plane C3 associated with determining Δ.

Table 1. Optimized (M11/6-311+G(d,p)) Structural Parameters (Distances in Å, Angles in deg) for Backbone Atoms of Silatanes $RSi(OCH_2)_3N$ (R = H (1), *t*-Bu (2), CF_3 (3))[a]

	Si–O	O–C	C–N	Si–N	Si–C3	Δ
1	1.665	1.444	1.459	2.554	2.128	0.426
2	1.672	1.443	1.458	2.566	2.140	0.426
3	1.652	1.453	1.458	2.508	2.091	0.417
	O–Si–O		Si–O–C	O–C–N		C–N–C
1	104.1		109.6	111.8		111.8
2	103.6		110.0	111.9		111.9
3	105.8		108.1	111.5		112.2

[a]Parameters for which more than one observation was available are averaged. C3 denotes the least-squares plane containing the three nitrogen-bound carbon atoms.

N and Si–O distances, whereas electron-poorer **3** exhibits shorter Si–N and Si–O distances. The angle data trend appropriately with the distances: the longer Si–O distances in **2** give rise to compressed O–Si–O angles and expanded Si–O–C angles, whereas the opposite holds for **3**. The effect diminishes rapidly, in that the more distant C–N distances and O–C–N and C–N–C angles are nearly identical across the series.

Included in the table are values for Δ = *d*(Si–C3) − *d*(Si–N), where C3 is the calculated least-squares plane containing the three amine carbons, and Si–C3 is the normal vector from the silicon to the plane (Figure 2, right) We use Δ values as proxies for the degree and direction of pyramidality of the nitrogen atom. They are mathematically equivalent in magnitude to the length of the normal vector from the nitrogen to the plane defined by the three substituent atoms in free amines, which defines the degree of pyramidality. The sign of Δ defines the direction of pyramidality: Δ < 0 denotes an *endo* isomer, Δ > 0 an *exo* isomer, and Δ = 0 an essentially trigonal planar nitrogen atom. One sees for 1–3 that Δ values are positive and differ little, characterizing the *exo* geometry around nitrogen and emphasizing the stiffness of the cage. For context, Δ = 0.341 Å for NH_3 and 0.445 for $N(CH_3)_3$ at the M11/6-311+G(d,p) level; thus the nitrogen atom in the silatanes examined is nearly as pyramidal as that in $N(CH_3)_3$. It is apparent, if not surprising, that silatanes prepared experimentally will exhibit quite pyramidal *exo* geometries around nitrogen.

2. Highly Constrained Backbones. An extension of the "smaller ring" concept involves stiffening the O—C—C backbone chain in a silatrane so that the N—C—C angle cannot adopt a value small enough to allow preference for the *endo* conformer. Examples involving O—C═C backbones are well-known for cases where the C═C bond is part of an arene ring. However, the crystal structures of $PhSi(OC_6H_4)_3N$[46] and $(ClCH_2)Si(OC_6H_4)_3N$[47] exhibit *endo* geometries around nitrogen, suggesting that the O—C═C backbone in these is flexible enough to allow N–C–C angle compression.

We examined the possibility that incorporating a cyclopropyl ring into the backbone would constrain the resulting silatrane adequately (**4**, Figure 3 and Table 2). This proved unsuccessful,

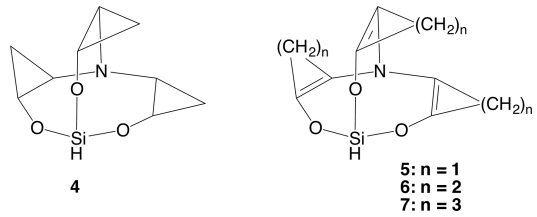

Figure 3. Skeleton pictures of **4**–**7**.

Table 2. Optimized (M11/6-311+G(d,p)) Structural Parameters (Distances in Å, Angles in deg) for Backbone Atoms of "Constrained Backbone" Silatranes 4–7[a]

	Si–O	O–C	C–C	C–N	Si–N	Si–C3	Δ
4	1.673	1.388	1.513	1.441	2.490	2.789	−0.299
5	1.677	1.348	1.287	1.439	3.680	3.066	0.614
6	1.663	1.358	1.333	1.427	3.365	2.982	0.383
7	1.676	1.357	1.331	1.422	2.678	2.777	−0.099
	O–Si–O		Si–O–C	O–C–C	C–C–N		C–N–C
4	115.5		128.6	116.2	112.8		115.8
5	109.2		119.9	145.5	139.1		103.1
6	109.7		124.7	133.6	132.1		113.1
7	114.2		126.6	124.4	119.1		119.5

[a]Parameters for which more than one observation was available are averaged. C3 denotes the least-squares plane containing the three nitrogen-bound carbon atoms.

in that molecule **4** optimizes to a structure with *endo* geometry around nitrogen, as shown by the short Si–N distance and the significantly negative Δ value. Comparing values with recently published computational data,[16] it appears that the O–Si–O and Si–O–C angles expand significantly compared to a typical silatrane containing a saturated backbone, lessening the structural effects associated with the atypical hybridization of the cyclopropyl carbon atoms.

To limit these angular expansions, we examined molecules **5**–**7**, combining the structural limitations imposed by small rings with those imposed by unsaturation in the backbone. As can be seen in Table 2, this proved effective in that the cyclopropenyl and cyclobutenyl silatranes **5** and **6** are predicted to exhibit *exo* pyramidal geometries at nitrogen. One sees that as the ring size increases from **5** to **7**, the Δ values rapidly become more positive, such that "cyclopentenyl backbone" silatrane **7** is predicted to adopt the *endo* geometry at nitrogen. Interestingly, although the Si–N distance changes dramatically across the series, the Si–O distances do not; the degree to which the silicon and nitrogen interact does not affect the degree to which the silicon and oxygens interact. This has been a point of considerable discussion.[2,48]

Scans of the potential energy surfaces associated with the Si–N distances for **5** and **6** demonstrated them to be single-minimum surfaces; structures exhibiting *endo* geometries at

DOI: 10.1021/acs.jpca.6b09346
J. Phys. Chem. A 2016, 120, 9315–9323

nitrogen were at least 50 kJ mol^{-1} less stable than the optimized *exo* versions. Synthesizing silatranes with such constrained backbones will undoubtedly prove difficult, but if they can be prepared, they should exhibit exclusively *exo* geometries at nitrogen, and so will represent examples of the "no Si−N bonding" extreme of the Si−N interaction spectrum.

3. Sterically Crowded Backbones. Inspection of structural models of silatranes shows that forming *endo* conformers engenders steric repulsions between the substituents on the nitrogen-bound carbon atoms greater than those in the *exo* conformers. One can envision exploiting this by substituting bulky moieties onto these positions (Figure 4).

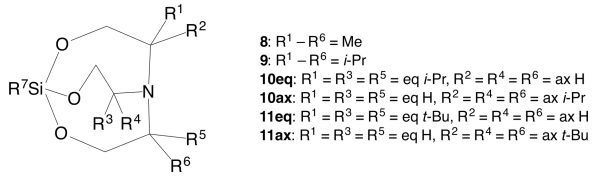

Figure 4. Skeleton picture of **8**−**11ax**.

Optimization of hexasubstituted **8** and **9** indicated potential success for this strategy, but the Δ values were ambiguous (Table 3). One sees that the M11 model predicts a slightly *exo* geometry for hexamethyl-substituted **8**, but the data are not reliable enough to distinguish this from the silatrane containing an essentially planar nitrogen atom. That said, this result was supported by the ωB97X-D model, for which Δ = 0.011. In contrast, hexaisopropyl-substituted **9** is predicted to adopt an *endo* structure at nitrogen, despite the increased steric bulk compared to that in **8**. Inspection of the structural data for **9** (Table 3) and visualization using the Mercury program suggests this occurs because isopropyl groups orient to minimize interactions between methyl groups, and because the backbone C−N bond lengths expand significantly over those in **8**. Gauged by the bond distance of 1.564 Å, the C−N bonds would likely be weak in such a molecule, possibly meaning it would not form, or would be rather unstable. We confirmed this somewhat by attempting to optimize the hexa-*tert*-butyl analogue of **9**; this molecule proved so crowded that the backbone C−N distances expanded beyond reasonable bonding values (>2 Å), making trustworthy optimization impossible.

While optimizing **9**, we noted that the bulky substituents forced the eight-membered rings to adopt conformations giving rise to stereodifferentiation at the nitrogen-bound carbon; by analogy to six-membered rings, we characterized the options as equatorial and axial (Figure 5). The observation led to the idea

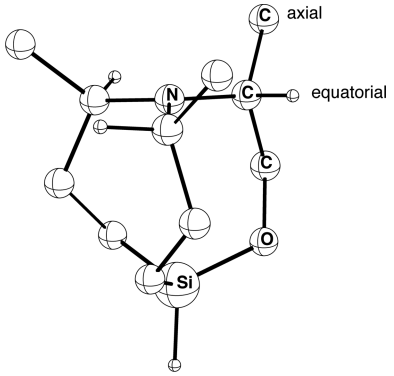

Figure 5. Skeleton picture of **11ax**, showing the axial *t*-Bu substituents (truncated to the tertiary carbon) and the equatorial H substituents. Methylene hydrogen atoms were removed for clarity.

that *tri*-equatorial and/or *tri*-axial substituted molecules might allow use of large substituents without engendering long C−N distances, and so might provide unambiguously *exo* geometries around nitrogen. Data for **10** and **11** in Table 3 bear this out; all four versions are predicted to exhibit C−N bonds of typical lengths. Substitution using isopropyl groups (**10eq**, **10ax**) at either position appears ineffective in providing *exo* geometries, in keeping with the results for **9**. However, substituting *tert*-butyl groups into the equatorial positions (**11eq**) gave an *exo* structure (albeit one only slightly different from one containing planar nitrogen (cf **9**)), whereas substituting *tert*-butyl groups into the axial positions (**11ax**) gave an unambiguously *exo* structure. Moreover, **11ax** proved significantly more stable than **11eq**, and so the more likely isomer formed if a tri-*tert*-butyl silatrane can be prepared. In this regard, we note that the trimethyl analogue of **11** (no equatorial/axial stereodifferentiation with the smaller methyl substituent) was prepared in 1999 using chiral trimethyltriethanolamine.[49] We thus anticipate that

Table 3. Optimized (M11/6-311+G(d,p)) Structural Parameters for Backbone Atoms (Distances in Å, Angles in deg) and Relative Energies (kJ mol^{-1}) for "Sterically Crowded Backbone" Silatranes 8−11[a]

	Si−O	O−C	C−C	C−N	Si−N	Si−C3	Δ
8	1.655	1.421	1.553	1.510	2.998	2.990	0.008
9	1.647	1.404	1.561	1.564	2.779	2.858	−0.079
10eq	1.657	1.422	1.552	1.471	2.869	2.950	−0.081
10ax	1.659	1.417	1.536	1.460	2.772	2.875	−0.103
11eq	1.651	1.425	1.552	1.479	3.054	3.027	0.027
11ax	1.647	1.424	1.546	1.492	3.308	3.074	0.232
	O−Si−O	Si−O−C	O−C−C	C−C−N	C−N−C		*E*
8	109.8	120.9	111.4	111.0	120.0		
9	114.2	133.8	114.6	110.4	119.8		
10eq	110.0	119.4	112.3	112.6	119.7		71
10ax	112.4	125.4	109.6	108.9	119.5		0
11eq	108.7	119.2	114.1	114.0	120.0		30
11ax	107.8	120.9	113.4	114.6	117.6		0

[a]Parameters for which more than one observation was available are averaged. C3 denotes the least-squares plane containing the three nitrogen-bound carbon atoms.

DOI: 10.1021/acs.jpca.6b09346
J. Phys. Chem. A 2016, 120, 9315−9323

11ax should prove preparable and will exhibit the *exo* geometry around nitrogen.

4. Lewis Acidity/Basicity Modifications. Silatranes adopt *endo* structures at nitrogen because this allows for the Lewis acidic silicon and Lewis basic nitrogen to interact via the nitrogen lone pair. Structural data generally indicate that the interaction is enhanced (as gauged by the Si−N distance) when the silicon is made more acidic and decreased when it is made less acidic. However, no silatrane has appeared where the silicon acidity is so low that the nitrogen adopts an *exo* geometry and does not interact with the silicon. One presumes that similar results would hold for the Lewis basicity of the nitrogen; silatranes containing particularly basic nitrogens (because the adjacent carbons have donating substituents) should exhibit Si−N distances shorter than those containing less basic nitrogens. Interestingly, the limited experimental data available conflict with this view.[49]

Stabilizing *exo* conformers by lowering the Lewis basicity of the nitrogen—possibly in tandem with lowering the Lewis acidity of silicon—does not appear to have been examined or exploited. Consequently, we examined silatranes **12**−**16**, containing various numbers and types of electron-withdrawing groups at the nitrogen-bound carbons and the same for electron-donating substituents on the silicon atoms.

The simplest silatranes consistent with this approach were the **12** series, with fluorines saturating the carbons adjacent to the nitrogen (Figure 6 and Table 4). The parent **12** exhibited a

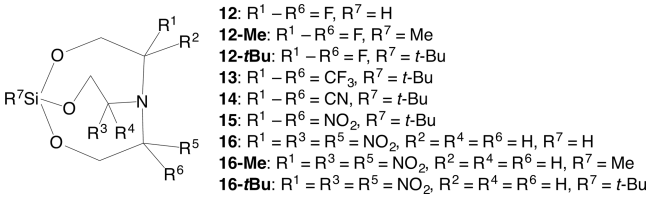

12: $R^1 - R^6 = F$, $R^7 = H$
12-Me: $R^1 - R^6 = F$, $R^7 = Me$
12-*t*Bu: $R^1 - R^6 = F$, $R^7 = t$-Bu
13: $R^1 - R^6 = CF_3$, $R^7 = t$-Bu
14: $R^1 - R^6 = CN$, $R^7 = t$-Bu
15: $R^1 - R^6 = NO_2$, $R^7 = t$-Bu
16: $R^1 = R^3 = R^5 = NO_2$, $R^2 = R^4 = R^6 = H$, $R^7 = H$
16-Me: $R^1 = R^3 = R^5 = NO_2$, $R^2 = R^4 = R^6 = H$, $R^7 = Me$
16-*t*Bu: $R^1 = R^3 = R^5 = NO_2$, $R^2 = R^4 = R^6 = H$, $R^7 = t$-Bu

Figure 6. Skeleton picture of **12**−**16-*t*Bu**.

miniscule preference for adopting the *exo* conformer, not clearly different from a case with nitrogen planar. It is notable that the predicted Si−N distance (2.961 Å) is *shorter* than that in methylated analogue **8**; Lewis acidity/basicity considerations would predict the reverse, because the nitrogen in **8** should be a far stronger base than the nitrogen in **12**. This supports the idea that steric bulk on carbons adjacent to the nitrogen can cause a preference for the *exo* geometry. To explore the effect of lowering the Lewis acidity of the silicon, we examined **12-Me** and **12-tBu**, with donor alkyl substituents bound to the silicon. This appeared to slightly increase the preference for the *exo* geometry, but the effect was too small to be reliable.

Spurred by this modest success, we examined **13**−**15**, containing *tert*-butyl substituents on silicon to lower its acidity, and saturating the relevant carbon atoms with increasingly electron-withdrawing substituents. The bond distances and angles for the three do not trend in any obvious way, save that the C−C distances decrease with the electron-withdrawing capacity of the substituent. Nonetheless, the trend in Si−N and Si−C3 distances is distinct: the former increase far more rapidly than the latter, such that **15** is predicted to adopt the *exo* geometry, whereas **13** and **14** adopt *endo* ones. It appears that modifying the Lewis acidities/basicities of the silicon and nitrogen atoms can force change from *endo* to *exo* geometry, but only if the modification changes the acidities/basicities

Table 4. Optimized (M11/6-311+G(d,p)) Structural Parameters for Backbone Atoms (Distances in Å, Angles in deg) for "Electronically Modified Backbone" Silatranes 12−17[a]

	Si−O	O−C	C−C	C−N	Si−N	Si−C3	Δ
12	1.656	1.409	1.531	1.449	2.961	2.953	0.008
12-Me	1.662	1.408	1.531	1.449	3.004	2.980	0.024
12-tBu	1.664	1.408	1.531	1.449	2.991	2.973	0.018
13	1.657	1.388	1.588	1.517	2.787	2.870	−0.083
14	1.670	1.399	1.577	1.475	2.875	2.983	−0.108
15	1.661	1.403	1.545	1.471	3.118	3.002	0.116
16	1.654	1.407	1.534	1.458	2.970	2.990	−0.020
16-Me	1.660	1.405	1.534	1.456	3.012	3.016	−0.004
16-tBu	1.662	1.405	1.534	1.457	2.997	3.008	−0.011
17	1.660	1.417	1.532	1.428	2.838	2.689	0.149

	O−Si−O	Si−O−C	O−C−C	C−C−N	C−N−C
12	109.1	126.2	109.0	114.5	120.0
12-Me	108.2	126.2	109.2	114.7	120.0
12-tBu	108.5	126.1	109.2	114.7	120.0
13	111.6	137.7	111.5	109.7	119.7
14	108.6	126.3	107.7	109.3	119.5
15	107.0	127.9	107.9	115.3	119.4
16	108.3	123.1	112.7	115.3	120.0
16-Me	107.4	123.4	112.9	115.6	120.0
16-tBu	107.7	123.2	112.9	115.5	120.0
17	108.2	127.6	110.5	114.0	118.9

[a]Parameters for which more than one observation was available are averaged. C3 denotes the least-squares plane containing the three nitrogen-bound carbon atoms.

significantly. In particular, it appears that the basicity of the nitrogen must be lowered drastically to cause it to avoid interaction with the silicon atom.

To probe this further, we examined the **16** series of silatranes, with three nitro substituents rather than six, analogous to the alkyl-substituted silatranes above but without axial/equatorial differentiation owing to the small size of the nitro group. It can be seen that all three homologues are predicted to exhibit nearly planar nitrogen atom geometries, with little differentiation between the overall structures. This reinforces the view that the basicity of the nitrogen must be reduced significantly to remove the Si−N interaction.

We identified two alternative approaches to accomplishing significant nitrogen basicity reduction. The first involves placing carbonyl functions adjacent to it, as in silatrane **17** (Figure 7). The carbonyl has the capacity to reduce nitrogen basicity via electron withdrawal. The data (Table 4) clearly indicate that **17** would exhibit the *exo* geometry at nitrogen. It is notable that the bond distances and angles in **17** differ little from those of the **16** series, yet none of the latter are clearly predicted to adopt *exo* geometries. This highlights our general observation

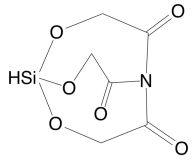

17

Figure 7. Skeleton picture of silatrane **17**.

DOI: 10.1021/acs.jpca.6b09346
J. Phys. Chem. A 2016, 120, 9315−9323

that no structural markers involving the backbone atoms exist that differentiate between *exo* and *endo* conformers. For example, one might anticipate that *endo* isomers would exhibit smaller C−C−N angles than *exo* isomers; the tabulated data do not strongly support this. Surprisingly, even the Si−N distance (within limits) is not a marker; note that this distance is smaller for **17** than for any members of the **16** series. This reflects the fact that the backbone atoms can adopt a range of torsional angles that in turn affect the Si−N distances. Indeed, the Si−N data for the **16** series make clear that even Si−N distances of *ca.* 3 Å (a value that approaches the sum of the Si and N van der Waals radii) do not guarantee that the silatrane nitrogen will adopt an *exo* geometry. It seems that even at this sizable distance, the two atoms have the ability to interact.

The second approach employs ammonium cations bound to the carbons adjacent to nitrogen to lower its basicity. We compared the structures of all permutations of substitution of amines/ammonium ions, as shown in Figure 8 and Table 5.

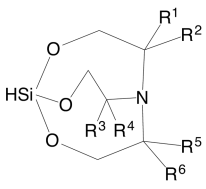

18: $R^1 = NH_2$, $R^2 - R^6 = H$
18H+: $R^1 = NH_3^+$, $R^2 - R^6 = H$
19: $R^1 = R^3 = NH_2$, R^2, $R^4 - R^6 = H$
19H+: $R^1 = NH_3^+$, $R^3 = NH_2$, R^2, $R^4 - R^6 = H$
19H+2: $R^1 = R^3 = NH_3^+$, R^2, $R^4 - R^6 = H$
20: $R^1 = R^3 = R^5 = NH_2$, $R^2 = R^4 = R^6 = H$
20H+: $R^1 = NH_3^+$, $R^3 = R^5 = NH_2$, $R^2 = R^4 = R^6 = H$
20H+2: $R^1 = R^3 = NH_3^+$, $R^5 = NH_2$, $R^2 = R^4 = R^6 = H$
20H+3: $R^1 = R^3 = R^5 = NH_3^+$, $R^2 = R^4 = R^6 = H$

Figure 8. Skeleton picture of **18**−**20H+3**.

Table 5. Optimized (M11/6-311+G(d,p)) Si−N and Si−C3 Distances and Δ Values (Å) for "Amine/Ammonium Backbone" Silatranes 18−20H+3[a]

	Si−N	Si−C3	Δ
18	2.512	2.785	−0.273
18H+	3.037	2.983	0.054
19	2.576	2.818	−0.242
19H+	3.031	2.985	0.046
19H+2	3.209	3.039	0.170
20	2.502	2.750	−0.248
20H+	2.667	2.850	−0.183
20H+2	3.117	2.993	0.124
20H+3	3.342	3.094	0.248

[a]C3 denotes the least-squares plane containing the three nitrogen-bound carbon atoms.

The data show interesting trends. For example, the Si−N distance does not change smoothly with increased NH_2-substitution for the mono-, di-, and tri-NH_2-substituted series **18**, **19**, and **20**. Moreover, the associated Δ values are nearly identical. This again suggests that changing the basicity of the backbone nitrogen atom has little impact on the Si−N distance or on Δ unless the change is significant. All three silatranes are predicted to adopt unmistakably *endo* geometries. Protonation of the amines to form ammonium ions results in the requisite change in basicity: **18H+**, **19H+**, and **19H+2** are predicted to adopt *exo* geometries, with the last being a particularly stark example. The trend for the **20** series reveals the competition between amine and ammonium: **20H+**, containing two amines and one ammonium, should exhibit an *endo* geometry, whereas **20H+2**, with the reverse ratio, should exhibit an *exo* geometry.

This dichotomy could plausibly allow **20** to act as a pH sensor. One envisions a substituent bound to silicon that responds detectably to the presence of an Si−N interaction, possibly an alkoxide or thiol that would undergo a substantial π-donating-based geometry change as the silicon changes from five-coordinate (including the Si−N interaction) to four-coordinate. Alternatively, the signal detected could arise from the silicon: it is known that five-coordinate silatranes exhibit ^{29}Si NMR chemical shifts at higher field than do four-coordinate triethoxysilanes.[2] As the pH decreases, the amines on **20** should become protonated; at some point, the **20H+** formed should be converted to **20H+2**, the silicon will become four-coordinate, and whatever signal associated with the five-coordinate silicon one monitors will vanish. At this point, the backbone nitrogen becomes a candidate for protonation, because the lone pair points "away" from the backbone; we did not explore whether this protonation would be preferred to formation of **20H+3**. On the basis of basicities, it probably would be, because the backbone nitrogen is tertiary; this might be countered if desired by using NMe_2 substituents on the backbone rather than NH_2 substituents.

Given the changes in Δ along the series, it might be possible to observe a change in signal between **20** and **20H+**, and between **20H+2** and **20H+3**, expanding the range and utility of the sensor. It is worth noting that silatrane itself exhibits good solubility in a range of solvents,[50] including water,[51] and reacts only slowly with weak acids.[52] Silicon-substituted silatranes are known to exhibit impressive hydrolytic stability;[53] hydrolyses of a variety of these in neutral solution or weak acid have been studied experimentally[5b,54,55] and computationally.[56,57]

5. QTAIM Data. Several electron localization models have been used to address the question of whether the silicon and nitrogen atoms in *endo*-silatranes are bonded.[2,48,58] The QTAIM approach has typically found Si−N bond paths (BPs,

Table 6. QTAIM Data (M11/pcseg-3) for Various Silatranes[a]

	Ex/En/Pl	Si−N	Δ	ρ(Si−N)	BPL	ρ (NB)	NB
8	Ex/Pl	3.000	0.024	0.015	3.000	0.017	H−H
12	Ex/Pl	2.953	0.018	n/a			
16	En/Pl	2.968	−0.006	n/a			
16-Me	Ex/Pl	3.012	0.010	n/a			
17	Ex	2.824	0.158	n/a			
18	En	2.606	−0.215	0.027	2.606		
18H+	Ex	3.022	0.061	n/a			

[a]Ex/En/Pl (exo/endo/planar) is the characterization of the nitrogen geometry based on Δ values. Si−N and Δ are defined as above. ρ(Si−N) is the electronic charge density at the bond critical point between the Si and N atoms; n/a means no Si−N BCP was found. BPL is the bond path length (Å). ρ(NB) is the electronic charge density at the bond critical point located between nonbonded peripheral atoms; NB indicates the nonbonding atom types.

DOI: 10.1021/acs.jpca.6b09346
J. Phys. Chem. A 2016, 120, 9315−9323

lines of maximum charge density linking nuclear critical points) and Si−N bond critical points (BCPs, points of maximum electron density along the bond path), and in some cases the ρ (electronic charge density) values at the BCPs are fairly large given that the distance between atoms is greater than the sum of the covalent bonding radii.[58,59] Keeping in mind that *exo*-silatranes retain some nitrogen lone pair electron density within the cage (in VSEPR terms, the smaller lobe of the nitrogen lone pair sp^3 orbital), and thus some Si−N interaction might exist in "planar nitrogen" silatranes or in *exo*-silatranes, it seemed worthy to examine some of each using QTAIM calculations. We refer the reader to the Computational Methods section for a caveat regarding the results.

The data in Table 6 suggest that "planar nitrogen" silatranes (**8**, **12**, **16**, and **16-Me**) have no Si−N bonding interactions, as evidenced either by the absence of Si−N BCPs or by exhibiting BCPs with ρ as small as that of a conventional nonbonding interaction (**8**). A fine line exists between no interaction and some interaction as characterized by ρ values; one sees that **18**, clearly *endo* by Δ value, exhibits $\rho = 0.027$, only slightly larger than the cutoff given in the Computational Methods section. It is notable that no Si−N BCP was located for trioxo **17**, consistent with the Δ value but possibly not with the relatively short Si−N distance (compare with **8**). Overall, the data support the view that silatrane Si−N interactions weaken significantly with distance, but correlating interaction strength with distance is challenging. Values of $\rho < 0.02$ are probably meaningless in characterizing Si−N interactions. It does not appear that the small lobe of the nitrogen lone pair orbital has the radial extent to interact well with the silicon.

CONCLUSIONS

The computational data, though oriented toward providing synthetic chemists with cage-based targets that would ultimately produce *exo* silatranes, provide several physical insights into the Si−N interaction and the geometry around the nitrogen atom in silatranes, and their ramifications. Foremost is that no thermochemical reason exists that *exo*-silatranes cannot be prepared. In fact, that we could not find any silatrane exhibiting a double-minimum potential energy surface implies that an *exo*-silatrane, if formed, will not readily isomerize to the *endo* form. It appears that the lack of observed *exo*-silatranes arises largely from lack of effort, and the difficulty in synthesizing the organic molecules that create the cage. The computational data suggest achievable, if challenging, target molecules, such as the sterically crowded **11ax**, for which related literature precedent exists. Derivatives of triamine silatrane **20** appear to be plausible targets that after multiple protonations should provide *exo*-silatranes. The constrained ring silatranes **5** and **6** are less viable, although the stability of the "arene backbone" versions mentioned provides hope that **6** might prove preparable.

A second insight involves determination that the "tipping point" of viable Si−N interaction is an Si−N distance of *ca.* 3.0 Å. Beyond this value, QTAIM models do not locate Si−N bond critical points, and the geometry around nitrogen is either planar or inverted with respect to the nitrogen lone pair pointing toward silicon. The tipping point value is some 0.5 Å shorter than the sum of the van der Waals radii for the two atoms, indicating that using the sum as a proxy for the presence/absence of an Si−N interaction is questionable.

In this regard, we were surprised to find that no structural marker we examined outside of Δ distinguishes *exo*- from *endo*-silatranes. On the basis of structural models and concepts of angle deformation, one might imagine discernible changes in distances and angles between the two; we noted the possibility that *endo* isomers would exhibit smaller C−C−N angles than *exo* isomers above. The data collected here indicate that this does not hold. This supports the view that, up to the 3.0 Å tipping point, the silicon and nitrogen atoms interact because the interaction stabilizes the molecule more than angle deformations destabilize it.

A third insight is that the Si−N interaction is sufficiently weak that placing bulky *tert*-butyl substituents adjacent to nitrogen (as in **11ax**) causes the nitrogen geometry to switch from *endo* to *exo*, despite the fact that such substitution makes the nitrogen atom more Lewis basic. It is understood that steric demands of substituents affect the ability of Lewis acid/base central atoms to interact (the field of frustrated Lewis pair chemistry[60] is based on the principle), but it is nonetheless interesting to observe the presence of bulky substituents causing inversion of geometry around the nitrogen. It is possible, though highly speculative, that this observation means that maximum Si−N interaction energy in a silatrane is equivalent to the repulsion energy associated with the *tert*-butyl substituents. However, we are unaware of an appropriate determination of the latter value, and unsure that it would apply to **11ax** if it exists.

Finally, it appears that it might be easier to observe the elusive planar nitrogen atom in a cage compound like a silatrane rather than in an acyclic amine. The computational data reinforce prior observations that silatranes have singular conformational minima: either the *endo* or *exo* isomer exists, but no potential energy surface exhibits both as minima. That we observed silatranes with nearly planar nitrogen atoms supports this as a phenomenon; presumably an NC_3 torsional vibration exists that oscillates between *endo* and *exo* isomers but does not occupy a well on each side sufficiently deep to allow for separable bond stretch isomers. That said, a synthesized silatrane containing planar nitrogen would be of considerable interest from experimental, spectroscopic, and theoretical standpoints. Possibly the rigidity of the silatrane cage will prove more able to stabilize the near-diradical nitrogen atom.

ASSOCIATED CONTENT

Supporting Information

The Supporting Information is available free of charge on the ACS Publications website at DOI: 10.1021/acs.jpca.6b09346.

Complete GAMESS and Gaussian 09 references, optimized (M11/6-311+G(d,p)) Cartesian coordinates and absolute energies for all molecules examined, Si−N/Si−C3/Δ values using various model chemistries, relative energies of the **10** and **11** series of silatranes, and QTAIM data using M11/various basis set model chemistries (PDF)

AUTHOR INFORMATION

Corresponding Author

*T.M.G. Telephone: 815-753-6896. E-mail: tgilbert@niu.edu.

Notes

The authors declare no competing financial interest.

ACKNOWLEDGMENTS

The NIU Computational Chemistry Laboratory is supported in part by the taxpayers of the state of Illinois.

DOI: 10.1021/acs.jpca.6b09346
J. Phys. Chem. A 2016, 120, 9315−9323

REFERENCES

(1) Pestunovich, V.; Kirpichenko, S.; Voronkov, M. In *The chemistry of organic silicon compounds*; Rappaport, Z., Apeloig, Y., Patai, S., Eds.; Wiley: New York, 1998; Vol. 2, pp 1447−1537.

(2) Puri, J. K.; Singh, R.; Chahal, V. K. Silatranes: a review on their synthesis, structure, reactivity and applications. *Chem. Soc. Rev.* **2011**, *40*, 1791−1840.

(3) Lyssenko, K. A.; Korlyukov, A. A.; Antipin, M. Y.; Knyazev, S. P.; Kirin, V. N.; Alexeev, N. V.; Chernyshev, E. A. The nature of the intramolecular transannular Si···N interaction in crystalline 1-methylsilatrane, as found from X-ray diffraction data. *Mendeleev Commun.* **2000**, *10*, 88−90.

(4) Trofimov, A. B.; Zakrzewski, V. G.; Dolgounitcheva, O.; Ortiz, J. V.; Sidorkin, V. F.; Belogolova, E. F.; Belogolov, M.; Pestunovich, V. A. Silicon-nitrogen bonding in silatranes: assignment of photoelectron spectra. *J. Am. Chem. Soc.* **2005**, *127*, 986−995.

(5) Hencsei, P.; Parkanyi, L. The molecular structure of silatranes. *Reviews on Silicon, Germanium, Tin and Lead Compounds* **1985**, *8*, 191−218.

(6) Voronkov, M. G.; D'yakov, V. M.; Kirpichenko, S. V. Silatranes. *J. Organomet. Chem.* **1982**, *233*, 1−147.

(7) Karlov, S. S.; Tyurin, D. A.; Zabalov, M. V.; Churakov, A. V.; Zaitseva, G. S. Quantum chemical study of group 14 elements pentacoordinated derivatives − metallatranes. *J. Mol. Struct.: THEOCHEM* **2005**, *724*, 31−37.

(8) Belyakov, S.; Ignatovich, L.; Lukevics, E. Concerning the transannular bond in silatranes and germatranes: a quantum chemical study. *J. Organomet. Chem.* **1999**, *577*, 205−210.

(9) Schmidt, M. W.; Windus, T. L.; Gordon, M. S. Structural trends in silicon atranes. *J. Am. Chem. Soc.* **1995**, *117*, 7480−7486.

(10) (a) Shishkov, I. F.; Khristenko, L. V.; Rudakov, F. M.; Golubinskii, A. B.; Vilkov, L. V.; Karlov, S. S.; Zaitseva, G. S.; Samdal, S. Molecular structure of silatrane determined by gas electron diffraction and quantum-mechanical calculations. *Struct. Chem.* **2004**, *15*, 11−16.

(11) Gordon, M. S.; Carroll, M. T.; Jensen, J. H.; Davis, L. P.; Burggraf, L. W.; Guidry, R. M. Nature of the Si-N bond in silatranes. *Organometallics* **1991**, *10*, 2657−60.

(12) Csonka, G. I.; Hencsei, P. Prediction of geometrical parameters for silatranes: an *ab initio* molecular orbital and density functional theory study. *J. Mol. Struct.: THEOCHEM* **1996**, *362*, 199−208.

(13) Labinger, J. A. Bond-stretch isomerism: a case study of a quiet controversy. *C. R. Chim.* **2002**, *5*, 235−244.

(14) Rohmer, M.-M.; Benard, M. Bond-stretch isomerism in strained inorganic molecules and in transition metal complexes: a revival? *Chem. Soc. Rev.* **2001**, *30*, 340−354.

(15) Parkin, G. Bond-stretch isomerism in transition metal complexes: a reevaluation of crystallographic data. *Chem. Rev.* **1993**, *93*, 887−911.

(16) Marin-Luna, M.; Alkorta, I.; Elguero, J. Theoretical study of the geometrical, energetic and NMR properties of atranes. *J. Organomet. Chem.* **2015**, *794*, 206−215.

(17) Sidorkin, V. F.; Doronina, E. P. Cage Silaphosphanes with a P → Si dative bond. *Organometallics* **2009**, *28*, 5305−5315.

(18) Boese, R.; Blaser, D.; Antipin, M. Y.; Chaplinski, V.; de Meijere, A. Non-planar structures of Et_3N and Pr^i_3N: a contradiction between the X-ray, and NMR and electron diffraction data for Pr^i_3N. *Chem. Commun.* **1998**, 781−782.

(19) Bock, H.; Goebel, I.; Havlas, Z.; Liedle, S.; Oberhammer, H. Triisopropylamine, a sterically crowded molecule with a flattened NC_3 pyramid and p-type electron pair. *Angew. Chem., Int. Ed. Engl.* **1991**, *30*, 187−90.

(20) Yang, M.; Albrecht-Schmitt, T.; Cammarata, V.; Livant, P.; Makhanu, D. S.; Sykora, R.; Zhu, W. Trialkylamines more planar at nitrogen than triisopropylamine in the solid state. *J. Org. Chem.* **2009**, *74*, 2671−2678.

(21) Koelmel, C.; Ochsenfeld, C.; Ahlrichs, R. An ab initio investigation of structure and inversion barrier of triisopropylamine and related amines and phosphines. *Theor. Chim. Acta* **1992**, *82*, 271−84.

(22) Schmidt, M. W.; Baldridge, K. K.; Boatz, J. A.; Elbert, S. T.; Gordon, M. S.; Jensen, J. H.; Koseki, S.; Matsunaga, N.; Nguyen, K. A.; et al. General atomic and molecular electronic structure system. *J. Comput. Chem.* **1993**, *14*, 1347−1363.

(23) Gordon, M. S; Schmidt, M. W. In *Theory and Applications of Computational Chemistry, the first forty years*; Dykstra, C. E., Frenking, G., Kim, K. S., Scuseria, G. E., Eds.; Elsevier: Amsterdam, 2005; pp 1167−1189.

(24) Frisch, M. J.; Trucks, G. W.; Schlegel, H. B.; Scuseria, G. E.; Robb, M. A.; Cheeseman, J. R.; Scalmani, G.; Barone, V.; Mennucci, B.; Petersson, G. A.; et al. *Gaussian 09*, Revision E.01; Gaussian, Inc.: Wallingford, CT, 2013.

(25) Zhao, Y.; Truhlar, D. G. The M06 suite of density functionals for main group thermochemistry, thermochemical kinetics, noncovalent interactions, excited states, and transition elements: two new functionals and systematic testing of four M06-class functionals and 12 other functionals. *Theor. Chem. Acc.* **2008**, *120*, 215−241.

(26) Peverati, R.; Truhlar, D. G. Improving the accuracy of hybrid meta-GGA density functionals by range separation. *J. Phys. Chem. Lett.* **2011**, *2*, 2810−2812.

(27) Chai, J.-D.; Head-Gordon, M. Long-range corrected hybrid density functionals with damped atom−atom dispersion corrections. *Phys. Chem. Chem. Phys.* **2008**, *10*, 6615−6620.

(28) Möller, C.; Plesset, M. S. Note on an approximation treatment for many-electron systems. *Phys. Rev.* **1934**, *46*, 618−622.

(29) Macrae, C. F.; Bruno, I. J.; Chisholm, J. A.; Edgington, P. R.; McCabe, P.; Pidcock, E.; Rodriguez-Monge, L.; Taylor, R.; van de Streek, J.; Wood, P. A. Mercury CSD 2.0 - new features for the visualization and investigation of crystal structures. *J. Appl. Crystallogr.* **2008**, *41*, 466−470.

(30) van Eikema Hommes, N. *Molecule for Macintosh*, Version 1.3.5d9; University of Erlangen-Nürnberg: Erlangen, Germany, 1999.

(31) Keith, T. A. *AIMAll*, Version 12.06.03; TK Gristmill Software: Overland Park, KS, 2012.

(32) Bader, R. F. W. *Atoms in Molecules: A Quantum Theory*; Oxford University Press: Oxford, U.K., 1990.

(33) Bader, R. F. W. A quantum theory of molecular structure and its applications. *Chem. Rev.* **1991**, *91*, 893−928.

(34) Bader, R. F. W. Atoms in molecules. *Acc. Chem. Res.* **1985**, *18*, 9−15.

(35) Cartesian basis functions were employed because early releases of the QTAIM programs required them, and because we have previously observed that AIMAll sometimes gives anomalous QTAIM results when spherical basis set-based wave functions are used.

(36) Woon, D. E.; Dunning, T. H., Jr. Gaussian basis sets for use in correlated molecular calculations. III. The atoms aluminum through argon. *J. Chem. Phys.* **1993**, *98*, 1358−1371.

(37) Kendall, R. A.; Dunning, T. H., Jr.; Harrison, R. J. Electron affinities of the first-row atoms revisited. Systematic basis sets and wave functions. *J. Chem. Phys.* **1992**, *96*, 6796−6806.

(38) Dunning, T. H., Jr. Gaussian basis sets for use in correlated molecular calculations. I. The atoms boron through neon and hydrogen. *J. Chem. Phys.* **1989**, *90*, 1007−1023.

(39) Jensen, F. Unifying general and segmented contracted basis sets. Segmented polarization consistent basis sets. *J. Chem. Theory Comput.* **2014**, *10*, 1074−1084.

(40) For context, the Si−N BCP ρ values in *endo*-silatranes are typically *ca.* 0.040, whereas the Si−O BCP ρ values are *ca.* 0.12, and all other X−Y BCP ρ values exceed that. This is in keeping with "general observation" values provided by Bader.[32]

(41) Defending this nomenclature: the term "silatrane" is a specific example of an "atrane", a term originally applied to a [3,3,3] octa-atom ring cage systems (neglecting any transannular interactions). Recently, however, the term "silatrane" was applied to cages composed of ten-membered rings,[43] and a recent publication suggested applying the term to a significantly wider range of molecules.[16] It seems appropriate

DOI: 10.1021/acs.jpca.6b09346
J. Phys. Chem. A 2016, 120, 9315−9323

to use a term with fewer letters, like atane in general and silatane for the case here, to describe a cage with fewer atoms.
(42) Ishmaeva, E. A.; Timosheva, A. P.; Gazizova, A. A.; Chachkov, D. V.; Vereshchagina, Y. A.; Kataev, V. E.; Timosheva, N. V. Dipole moments, structure, and transannular interactions in silatranes containing planar fragments. *Russ. J. Gen. Chem.* **2008**, *78*, 1350−1353.
(43) Timosheva, A. P.; Chandrasekaran, A.; Day, R. O.; Holmes, R. R. A new class of silatranes. *Phosphorus, Sulfur Silicon Relat. Elem.* **2001**, *168*, 59−68.
(44) Lian, H.; Li, Y.; Chen, J. Discriminant analysis of structure toxicity relations on silatranes. *Jisuanji Yu Yingyong Huaxue* **1988**, *5*, 36−42.
(45) Lagrange, A. Hair dye preparations containing direct dyes with disulfide/thiol protective group and silicon compounds with thiol group. PCT Int. Appl. 2009, WO 2009109457 A2 20090911.
(46) Boer, F. P.; Turley, J. W.; Flynn, J. J. Structural studies of pentacoordinate silicon. 11. Phenyl(2,2′,2″-nitrilotriphenoxy)silane. *J. Am. Chem. Soc.* **1968**, *90*, 5102−5105.
(47) Chen, B.; Wu, G.; Luo, Y. Structure of 1-chloromethyl-3, 4, 6, 7, 10, 11- tribenzo-2, 8, 9- trioxa-5-aza-1-silatricyclo[3.3.3. 01, 5]-undecane, ($C_{19}H_{14}ClNO_3Si$). *Jiegou Huaxue* **1987**, *6*, 165−168.
(48) Sidorkin, V. F.; Belogolova, E. F.; Doronina, E. P. Assignment of photoelectron spectra of silatranes: first ionization energies and the nature of the dative Si←N contact. *Phys. Chem. Chem. Phys.* **2015**, *17*, 26225−26237.
(49) Stachel, S. J.; Ziller, J. W.; Van Vranken, D. L. A Chiral C_3 Triisopropylamine and its silatrane derivatives. *Tetrahedron Lett.* **1999**, *40*, 5811−5812.
(50) Skrypai, V.; Hurley, J. J. M.; Adler, M. J. Silatrane as a practical and selective reagent for the reduction of aryl aldehydes to benzylic alcohols. *Eur. J. Org. Chem.* **2016**, *2016*, 2207−2211.
(51) Adler, M. J.; Gilbert, T. M.; Skrypai, V.; Varjosaari, S. E. Patent pending.
(52) Skrypai, V. Personal communication.
(53) Frye, C. L.; Vincent, G. A.; Finzel, W. A. Pentacoordinate silicon compounds. V. Novel silatrane chemistry. *J. Am. Chem. Soc.* **1971**, *93*, 6805−6811.
(54) Voronkov, M. G.; Toryashinova, D-S. D.; Baryshok, V. P.; Shainyan, B. A.; Broadskaya, E. I. Kinetics of hydrolysis of silatranes in a neutral medium. *Izv. Akad. Nauk SSSR Seri. Kimiches.* **1984**, *12*, 2673−2676.
(55) Frye, C. L.; Streu, R. D. Pentacoordinate silicon compounds. VII. Solvolysis of some phenyl silatranes in acetic acid. *Main Group Metal Chem.* **1993**, *16*, 217−221.
(56) Sok, S.; Gordon, M. S. A *dash* of protons: A theoretical study on the hydrolysis mechanism of 1-substituted silatranes and their protonated analogs. *Comput. Theor. Chem.* **2012**, *987*, 2−15 and references therein..
(57) Chernyshev, E. A.; Knyazev, S. P.; Kirin, V. N.; Vasilev, I. M.; Alekseev, N. V. Structural features of silatranes and germatranes. *Russ. J. Gen. Chem.* **2004**, *74*, 58−65.
(58) Korlyukov, A. A.; Lyssenko, K. A.; Antipin, M. Y.; Kirin, V. N.; Chernyshev, E. A.; Knyazev, S. P. Experimental and theoretical study of the transannular intramolecular interaction and cage effect in the atrane framework of boratrane and 1-methylsilatrane. *Inorg. Chem.* **2002**, *41*, 5043−5051.
(59) Korlyukov, A. A. Coordination compounds of tetravalent silicon, germanium and tin: the structure, chemical bonding and intermolecular interactions in them. *Russ. Chem. Rev.* **2015**, *84*, 422−440.
(60) Stephan, D. W. Discovery of frustrated Lewis pairs: Intermolecular FLPs for activation of small molecules. *Top. Curr. Chem.* **2012**, *332*, 1−44.

DOI: 10.1021/acs.jpca.6b09346
J. Phys. Chem. A 2016, 120, 9315−9323